

## Practical implementation of generalized pushover analysis for multimodal pushover analysis

\*Firat Soner Alici<sup>1)</sup>, Kaan Kaatsız<sup>2)</sup> and Haluk Sucuoğlu<sup>3)</sup>

<sup>1), 2), 3)</sup> *Department of Civil Engineering, METU, Ankara, Turkey*

<sup>1)</sup> [fsalici@metu.edu.tr](mailto:fsalici@metu.edu.tr)

### ABSTRACT

A generalized pushover analysis procedure was previously developed for estimating the inelastic seismic response of structures under earthquake ground excitations. The procedure consists of applying different generalized force vectors separately for each story to the structure in an incremental form with increasing amplitude, until an estimated target interstory drift demand is obtained. A generalized force vector is expressed as a combination of modal forces, and simulates the instantaneous force distribution acting on the system when the interstory drift at a given story reaches its maximum value during dynamic response to a seismic excitation. Each nonlinear static analysis under a generalized force vector activates all modes of a multi degree of freedom system, simultaneously. Correspondingly, inelastic actions develop in members with the contribution of all instantaneous modes in the nonlinear response range.

A practical implementation of the proposed generalized pushover analysis is presented in this study. The method is applied to a 12 story frame and a 20 story frame-wall system, and the results are obtained under six spectrum-compatible ground motions. First, it has been demonstrated that generalized pushover analysis is successful in estimating maximum member deformations and exact in determining member forces under a ground excitation with reference to nonlinear response history analysis. Then, it is shown that the results obtained from generalized pushover analysis by using the mean spectrum of six ground motions are almost identical to the mean of the results obtained from separate generalized pushover analyses under six ground motions. Moreover, these mean results are very close to the mean of the results obtained from six nonlinear response history analyses.

### 1. INTRODUCTION

The ease of application and conceptual simplicity of single mode conventional pushover analysis enables to develop multimodal pushover analysis procedures which supersede nonlinear response history analysis in practical application (Sasaki et al. 1998, Chopra and Goel 2002, Gupta and Kunnath 2000, Aydınoğlu 2003, Antoniou and Pinho 2004). Generally, these methods, except one, are adaptive. In adaptive methods,

---

<sup>1), 2)</sup> Research Assistant, Ph.D. Candidate

<sup>3)</sup> Professor

eigenvalue analysis is conducted at each step of load increment according to the formation of nonlinear deformations in the system. This approach removes the simplicity of pushover analysis procedure, and requires special programming or modification of the current analysis programs. On the other hand, in multimodal pushover analysis, results are obtained for each mode independently, and then the modal results are combined by statistical rules (SRSS or CQC) for combining elastic modal responses. There are several shortcomings in the modal combination of inelastic modal responses. They are approximate, and the internal forces obtained by statistical combinations exceed capacities, hence they require correction at each load increment.

In this study, a recently developed multimodal pushover analysis (Sucuoğlu and Günay, 2011) which accounts for the contribution of all significant modes to inelastic seismic response is described, and its practical implementation is developed. In this procedure, a set of pushover analyses are conducted by employing different generalized force vectors, derived for each story. Therefore, for an N story building, N number of pushover analyses is required. Each generalized force vector is derived as a different combination of modal lateral forces in order to simulate the effective lateral force distribution when the interstory drift at a selected story reaches its maximum value during seismic response. Pushover analysis of a story proceeds in a step-by-step manner until the target interstory drift value of that story is achieved. Target interstory drift in any story can be estimated from linear elastic response spectrum analysis by considering the equal displacement rule. The contribution of the first mode response can also be obtained from the solution of inelastic SDOF system response. This suggested procedure can be implemented by using any structural analysis software (SAP, OpenSees, Drain2D, etc.) which facilitate displacement controlled pushover analysis.

This study focuses on the practical implementation of generalized pushover analysis (GPA) which requires less computational effort. Performance of GPA and its practical implementation (RGPA) is compared with the benchmark nonlinear response history analysis, based on the results obtained from the analyses of a twelve story RC frame.

## 2. GENERALIZED PUSHOVER ANALYSIS

The generalized pushover procedure is based on an effective force vector  $\mathbf{f}_j$  acting on the system when the interstory drift  $\Delta_j$  at the  $j$ 'th story reaches its maximum value during dynamic response. This is a generalized force vector since it includes contributions from all modal forces at the time of maximum response of the interstory drift at the  $j$ 'th story. If this force vector is defined, it can then be applied to the system as an equivalent static force in order to produce the maximum value of the  $j$ 'th interstory drift. In GPA, generalized force vectors  $\mathbf{f}_j$  are derived from the dynamic response of linear elastic MDOF systems under earthquake ground excitations by using the response spectrum analysis (RSA) procedure.

$$\mathbf{f}_j = \sum_n \left( \Gamma_n \mathbf{m} \boldsymbol{\phi}_n A_n \frac{\Delta_{j,n}}{\Delta_{j,max}} \right) \quad (1)$$

Here,  $\Gamma_n = L_n/M_n$ ;  $L_n = \boldsymbol{\varphi}_n^T \mathbf{m} \mathbf{l}$ ;  $M_n = \boldsymbol{\varphi}_n^T \mathbf{m} \boldsymbol{\varphi}_n$ ;  $\boldsymbol{\varphi}_n$  is the  $n$ 'th mode shape;  $\mathbf{m}$  is the mass matrix,  $\mathbf{l}$  is the influence vector, and  $A_n$  is the spectral acceleration at the  $n$ 'th mode. In Eq. (1),  $\Delta_{j,n}$  is the  $n$ 'th mode contribution to the maximum interstory drift of the  $j$ 'th story determined from RSA, and  $\Delta_{j,max}$  is the quadratic combination of the spectral modal drift terms  $\Delta_{j,n}$  according to Eq. (2).

$$(\Delta_{j,max})^2 \approx \sum_n [\Gamma_n D_n (\varphi_{n,j} - \varphi_{n,j-1})]^2 \quad (2)$$

The target interstory drift demand  $\Delta_{jt}$  at the  $j$ 'th story can be obtained consistently with the generalized force vector  $\mathbf{f}_j$ ,

$$\Delta_{jt} = \sum_n \Gamma_n D_n \frac{\Delta_{j,n}}{\Delta_{j,max}} (\varphi_{n,j} - \varphi_{n,j-1}) \quad (3)$$

by invoking the modal scaling rule of GPA:

$$D_n(t_{max}) = D_n \frac{\Delta_{j,n}}{\Delta_{j,max}} \quad (4)$$

$D_n(t_{max})$  is the modal displacement amplitude at  $t_{max}$  which satisfies the equation of motion of the SDOF system representing the  $n$ 'th mode under a ground excitation  $\ddot{u}_g(t)$ , and  $D_n$  is the spectral displacement at the  $n$ 'th mode.  $D_n(t_{max})$  satisfies the equation of motion,

$$\ddot{D}_n(t_{max}) + 2\zeta_n \omega_n^2 \dot{D}_n(t_{max}) + \omega_n^2 D_n(t_{max}) = -\ddot{u}_g(t_{max}) \quad (5)$$

where  $t_{max}$  is the time when  $\Delta_j$  reaches its maximum value under  $\ddot{u}_g(t)$ . In order to improve the prediction of Eq. (3), the first mode linear elastic spectral displacement demand  $D_1$  can be replaced with the first mode inelastic spectral displacement demand  $D_1^*$ . This operation requires conducting an 'a priori' first mode pushover analysis. Then,  $D_1^*$  can be estimated from the nonlinear response history analysis of the equivalent SDOF system which is representing the first mode behavior.

GPA uses the higher-order interstory drift parameter as target demand rather than the lowest order story (roof) displacement parameter. Accordingly, when the associated generalized force vector  $\mathbf{f}_j$  pushes the system to the target drift  $\Delta_{jt}$ , the system adopts itself in the inelastic deformation range, and the first and second order deformation parameters (rotations and curvatures) and the second and third order force parameters (moments and shears) take their inelastic values with more effective contributions from the higher modes. On the other hand, if story (roof) displacement is used as target demand, the contribution of higher modes becomes less significant. If different local response parameters are primary considerations during inelastic dynamic response, interstory drift values are more effective representatives of local maximum response parameters as target deformation because they are well synchronized with

the local response parameters.

$N$  number of pushovers is conducted in GPA for each story sequentially. In the  $j$ th story GPA, the structural system is pushed incrementally with the force vector  $\mathbf{f}_j$ . Displacement controlled pushover analysis is conducted until  $\Delta_j$  reaches  $\Delta_{jt}$ . After completing all GPA from 1 to  $N$ , member deformations and member internal forces are determined by taking envelopes of the related GPA results, and these envelope values are registered as the maximum seismic response values.

### 3. REDUCTION IN THE NUMBER OF GENERALIZED PUSHOVERS: INSTANTS OF MAXIMUM RESPONSE

GPA is based on the general assumption that the interstory drift ratios  $\Delta_j$  occur independently at each story ( $j=1-N$ ) at different instants  $t_{j,max}$ ,  $j=1-N$ . However if there are  $n$  modes contributing significantly to the total dynamic response ( $n < N$ ), then there are only  $2^{(n-1)}$  possible combinations of the  $n$  modes leading to the maximum values of interstory drifts at specific stories. Hence there are  $2^{(n-1)}$  independent instants  $t_{max}$  for calculating  $\mathbf{f}_j$  and  $\Delta_{j,max}$  in the  $N$  DOF system.

The reduction concept in generalized pushover analysis is introduced herein with implementation to a 12-story reinforced concrete building having four identical frames and a symmetrical floor plan, shown in Fig. 1. The first three modal periods are 2.39, 0.82, and 0.48 seconds, respectively.

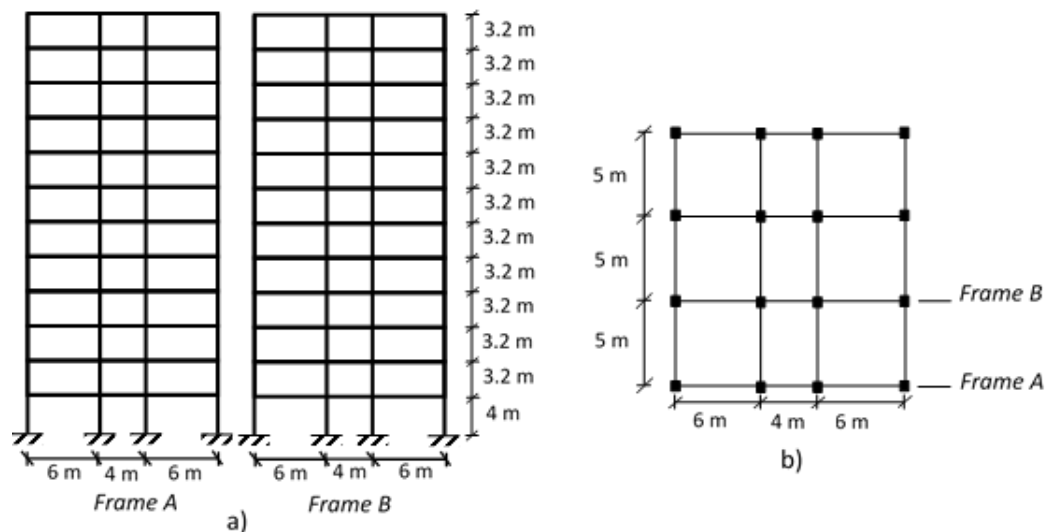


Fig. 1 a) Elevation, b) floor plan of the 12 story building

Let's consider the linear elastic spectral drift profiles of the first three modes for the 12-story RC frame under the CHY006-E strong motion component of the 1999 Chi-Chi earthquake shown below in Fig. 2.

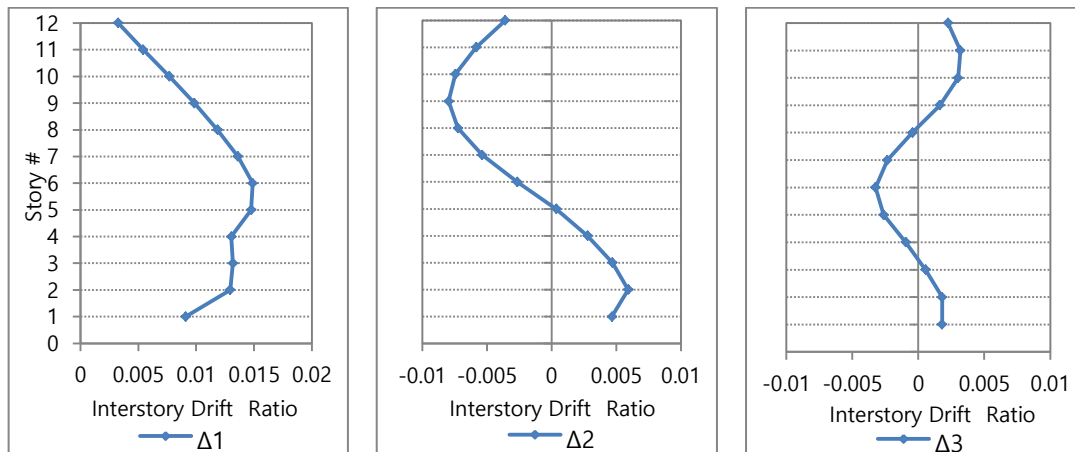


Fig. 2 Drift profiles for the first three modes under CHY006-E (drift ratios)

Here,

$$\Delta_{j,n} = [\Gamma_n D_n (\varphi_{n,j} - \varphi_{n,j-1})] \quad (6)$$

is the  $n$ 'th mode spectral drift ratio at the  $j$ 'th story, where  $D_n$  is obtained from the linear elastic response spectrum of CHY006-E. There are  $2^{(n-1)}$  possible combinations for  $n$  number of significant modes contributing to interstory drifts. For  $n=2$  and  $n=3$ , possible combinations are shown in Fig. 3 and Fig. 4, respectively. It should be noted that these are the absolute maximum combinations of modal drifts. During actual dynamic response, maximum modal drift distributions do not occur synchronously. However this situation does not affect the approach presented.

According to Fig. 3, the combinations  $\Delta_1 + \Delta_2$  and  $\Delta_1 - \Delta_2$  control the system in two ranges along its height, the lower 1<sup>st</sup>-5<sup>th</sup> stories and the upper 6<sup>th</sup>-12<sup>th</sup> stories, respectively. On the other hand, according to Fig. 4, different combinations of the first three modes control the system in four different ranges. Fig. 4 reveals that  $\Delta_1 - \Delta_2 + \Delta_3$  combination controls the upper (9<sup>th</sup>-12<sup>th</sup>) stories whereas  $\Delta_1 + \Delta_2 + \Delta_3$  combination controls the lower (1<sup>st</sup>-3<sup>rd</sup>) stories. For the middle stories,  $\Delta_1 + \Delta_2 - \Delta_3$  and  $\Delta_1 - \Delta_2 - \Delta_3$  combinations control the interstory drift maxima of the 4<sup>th</sup>-5<sup>th</sup>, and 6<sup>th</sup>-8<sup>th</sup> stories, respectively.

This condition is further established with the elastic time history analysis (ETHA) results. In Fig. 5, drift profiles are plotted when the interstory drift values in each range attain their maximum values during linear elastic dynamic response analysis under CHY006-E for the related four combinations of the first three modes. The control stories are selected as the 2<sup>nd</sup>, 5<sup>th</sup>, 7<sup>th</sup> and 11<sup>th</sup> from the first, second, third and fourth story ranges, respectively. The envelope of maximum interstory drift values obtained from ETHA by considering all 12 modes are also plotted on the same figure. It is clear from Fig. 5 that the maximum interstory drifts occur at four different instants with the drift profiles approximately shown in Fig. 4. The intention for such comparison is to show that the reduced number of pushovers (from 12 to 4) with the related force vectors would be sufficient to capture the maximum dynamic response of the system under a ground motion. When the second story interstory drift reaches its maximum, the first and the third stories also reach their maxima synchronously in the first range as shown

in Fig. 5. This is almost the case for the other ranges as well. The error at the ninth story is somewhat more significant, due to falling between two ranges.

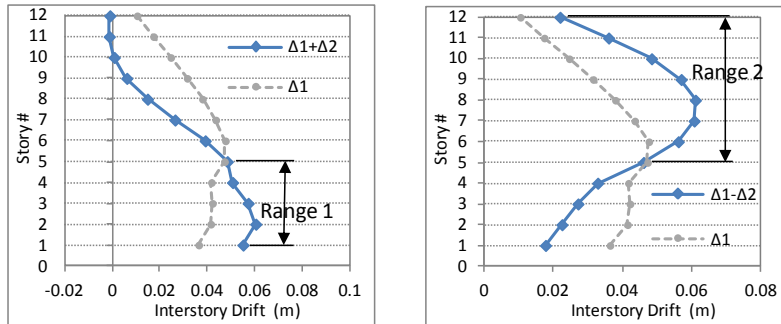


Fig. 3 Combinations of the first two modes contributing to interstory drift

Accordingly, one story level from each story range can be selected, and the associated four ( $2^{(n-1)}$ ,  $n=3$ ) force vectors can be employed in GPA instead of the  $N$  numbers of force vectors, i.e.,  $N$  number of generalized pushovers. The ranges are directly identified from the intercepts of the mode shapes as shown in Fig. 3 and Fig. 4. For the 12-story frame, considering the combinations of the first three modes, 2<sup>nd</sup>, 5<sup>th</sup>, 7<sup>th</sup> and 11<sup>th</sup> stories are selected from each story range (middle stories of each range), and only four generalized pushover analyses are conducted by applying  $f_2$ ,  $f_5$ ,  $f_7$  and  $f_{11}$  in accordance with Eq. (1). Finally, the envelopes of these four generalized pushover analyses are employed for calculating the maximum response parameters. Thus, the computation effort in GPA is considerably reduced from 12 to 4 pushovers for this case.

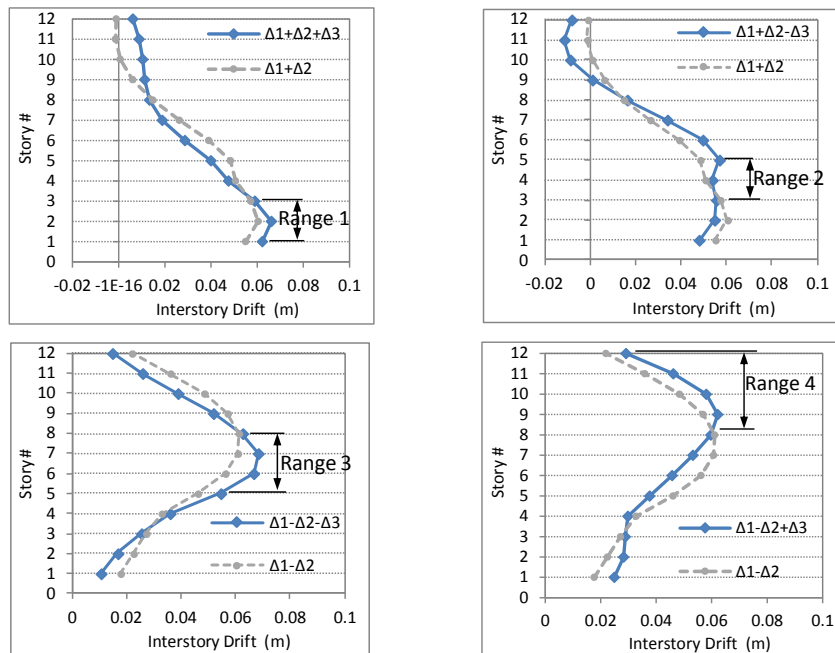


Fig. 4 Combinations of the first three modes contributing to interstory drift

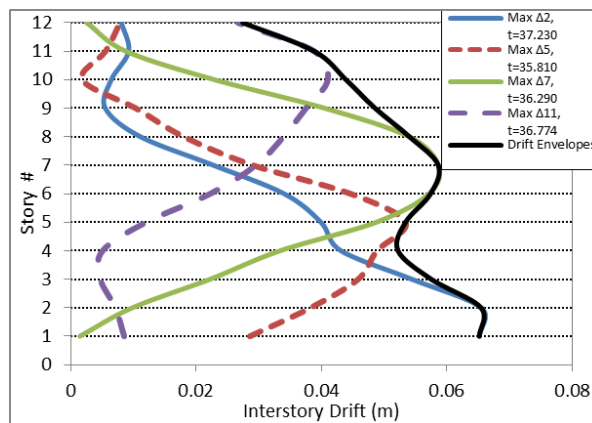


Fig. 5 Comparison of ETHA maximum drift envelope with the maximum drift profiles in four ranges

#### 4. GROUND MOTIONS EMPLOYED IN CASE STUDIES

The ground motion set employed in the case studies contains six different spectrum matched ground motions. Acceleration records of these six ground motions were generated from the selected reference data set of ground motions which have similar properties (Hancock and Bommer, 2006). The spectrum of each ground motion is adjusted with the Turkish Earthquake Code (TEC 2007) design spectrum. These reference ground motions were selected to be capable of generating higher mode effects on the structural systems, and downloaded from the PEER strong motion database (PEER, 2010). Important features of both the reference and the spectrum matched ground motions are presented in Table 1.

The spectrum matched synthetic ground motions were derived by using the RSPMatch2005 (Hancock et al. 2006) software program. The derivation process is based on changing the frequency range of the reference ground motion in order to match the original acceleration spectrum with the given target acceleration spectrum. Fig. 6 shows the acceleration spectra of synthetic ground motions, their mean spectrum and TEC (2007) design spectrum. Acceleration spectrum of the reference GM4, scaled by 1.5 is also added to Fig. 6. This ground motion is used to represent maximum seismic intensity in the following analysis.

Table 1 Properties of reference and spectrum matched ground motions

#	GM Code	Earthquake (Mw)	Station - Component	CD (km)	Site Geol.	PGA (g)		PGV (cm/s)		PGD (cm)	
						Ref.	Spect. matched	Ref.	Spect. matched	Ref.	Spect. matched
1	CLS090	Loma Prieta, 1989 (7)	Corralitos-090	3,9	A	0,479	0,449	45,2	53,2	11,3	20,3
2	LEX000	Loma Prieta, 1989 (7)	Lex. Dam-000	5,0	A	0,420	0,496	73,5	66,2	20,0	24,9
3	PCD254	San Fer., 1971 (6.6)	Pac. Dam-254	2,8	B	1,160	0,567	54,1	48,1	11,8	17,0
4	CHY006-E	Chi-Chi, 1999 (7.6)	CHY006-E	9,8	B	0,364	0,513	55,4	59,9	25,6	20,0
5	Bolu000	Duzce, 1999 (7.1)	Bolu-000	12,0	D	0,728	0,541	56,4	55,9	23,1	18,7
6	ERZ-EW	Erzincan, 19 92 (6.9)	Erzincan-EW	4,4	D	0,496	0,518	64,3	64,3	21,9	23,4

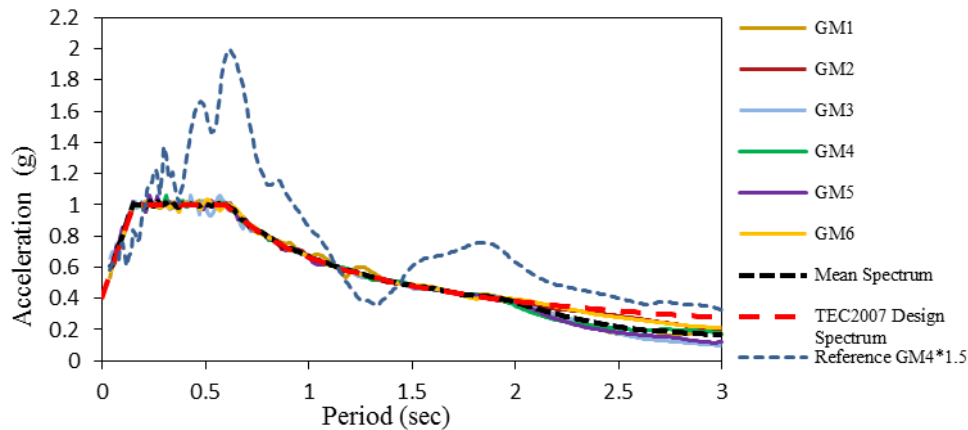


Fig. 6 Acceleration response spectrum matched ground motions, original GM4x1.5, mean acceleration spectrum, and TEC2007 design spectrum

## 5. COMPARATIVE RESULTS FROM CASE STUDIES

The reduced GPA procedure is employed in two case studies, a 12 story frame and a 20 story frame-wall system, both designed according to the capacity design principles for the design spectrum given in Fig. 6 and detailed according to the enhanced ductility requirements of the Turkish Earthquake Code (2007). Solutions are obtained under six ground motion components, and the results are evaluated in comparison with the results from nonlinear response history analysis.

Maximum interstory drifts, maximum average plastic rotations of beam ends in a story, maximum average chord rotations of column ends in a story, beam end moments and shear forces, column (shear wall) end moments and shear forces are obtained under the six ground motion components. Maximum average plastic or chord rotations at each story level are calculated by first averaging the member end rotations at the corresponding story at each load (or time) step, and then using the maximum of these values as the story maximum. The results of nonlinear response history analysis (NRHA), GPA and the reduced algorithm of generalized pushover analysis (RGPA) introduced herein are compared with each other for each ground motion in the set. The target drift in GPA is determined by employing the inelastic maximum displacement amplitude  $D_1^*$  for the first mode in Eq. (3).

### 5.1 Case Study I: Twelve Story RC Frame

The elevation and plan view of the frame were shown in Fig. 1. The member dimensions for beams are 300x550 mm for the first four stories, 300x500 mm for the second four stories, and 300x450 mm for the last four stories. The columns dimensions are 500x500 mm, 450x450 mm, and 400x400 mm in the first four, the second four, and the last four stories, respectively. The slab thickness is 140 mm, and live load is 3.5 kN/m<sup>2</sup>. Concrete and steel characteristic strengths are 25 MPa and 420 MPa, respectively.

Analytical model of the twelve story frame is generated by using the OpenSees software (2005). Structural frame members are modeled with “Beam with Hinges” element. For beam sections, bi-linear moment curvature relationships are defined along the hinge lengths by considering the designed section properties of each beam type. On the other hand, column sections are defined by utilizing fiber sections along the hinge lengths. The remaining part in between the plastic hinges of a member is defined with elastic section properties. In order to describe cracked section stiffness for each member, the gross moment of inertia values are multiplied by 0.4 and 0.6 for beams and columns respectively. Rigid diaphragms are assigned to each story level, and P- $\Delta$  effects are taken into account in the model. In time history analyses, Rayleigh damping is computed by considering 5% damping in the 1<sup>st</sup> and 3<sup>rd</sup> modes.

Maximum interstory drift ratios and maximum average beam-end plastic rotations are compared for the results of full GPA, RGPA and NRHA in Fig. 7 and Fig. 8, respectively. It can be observed from these figures that the results of RGPA are very close to those of the full GPA. However RGPA results deviate from the NRHA results by as much as 30% at the stories above the mid height where NRHA calculates higher plastic deformations due to the higher mode effects. The basic reason is the difference between the plastic hinge formation sequences of the two procedures. Nonlinear static procedures cannot perfectly simulate the sequence which occurs during actual dynamic response.

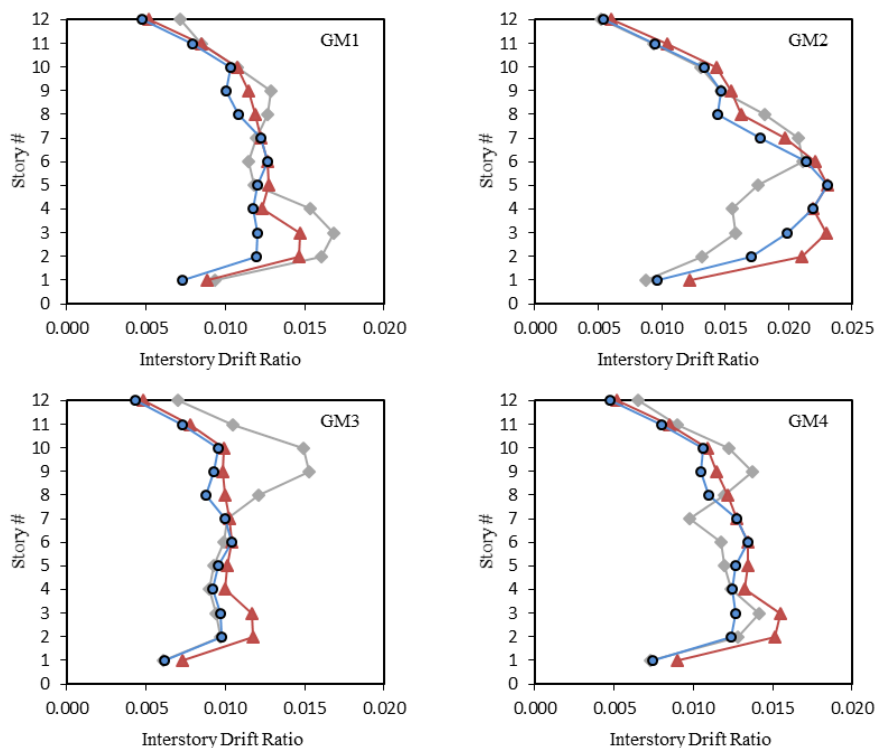


Fig. 7 Comparison of maximum interstory drift ratios obtained under six ground motions

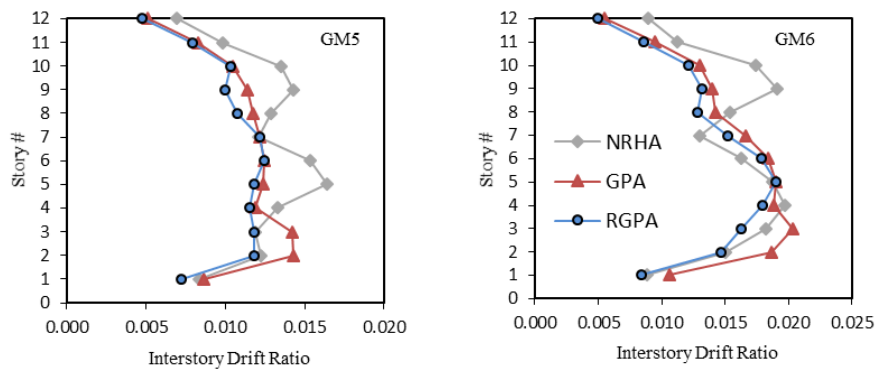


Fig. 7 Continued

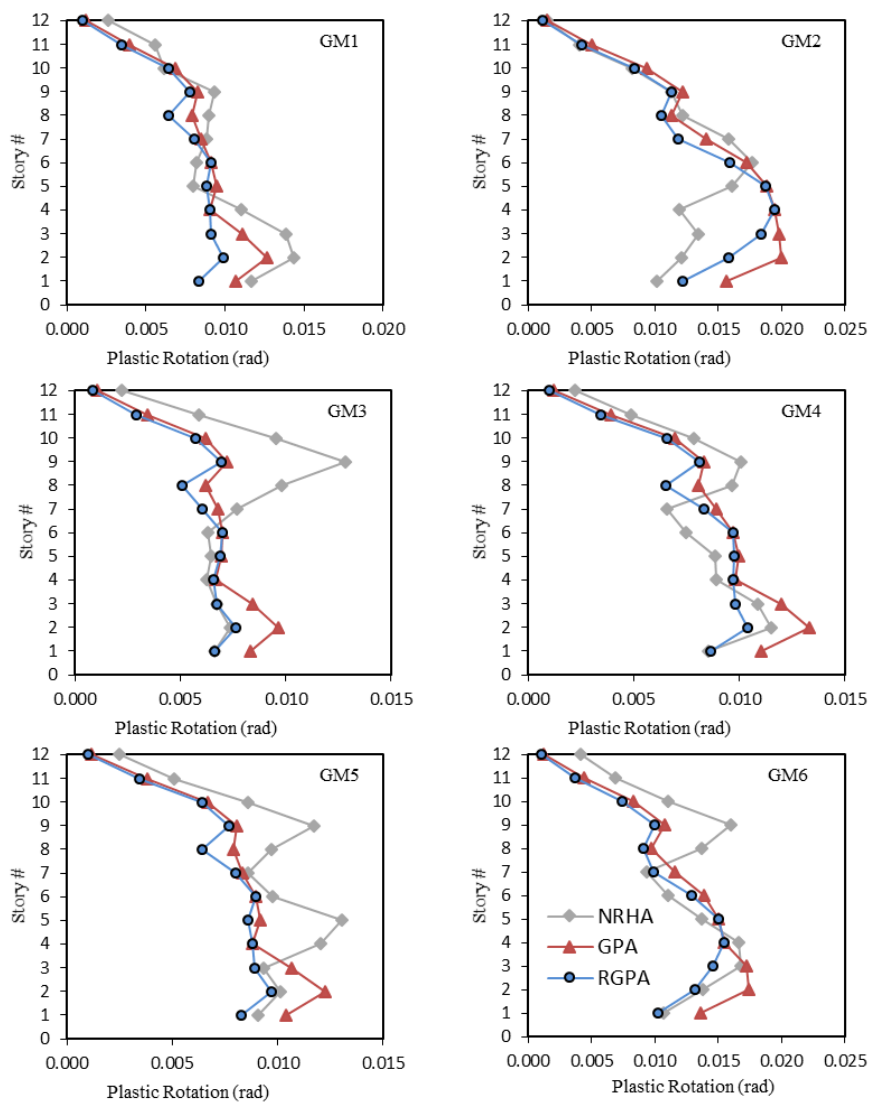


Fig. 8 Maximum values of average beam end plastic rotations under six ground motions

Since generalized pushover analysis is introduced with a reduction procedure in this study for practical implementation, only those results obtained with RGPA will be presented in the foregoing discussions and compared with the results of NRHA for verification.

Maximum beam-end plastic rotations at the 1<sup>st</sup>, 5<sup>th</sup>, and 10<sup>th</sup> stories, when plastic rotations at beam ends reach their maximum, are presented in Fig. 9 for five ground motions. Generally it can be observed that RGPA predicts NRHA results for plastic rotations quite well.

Maximum average column-end chord rotations at the first story column bases are shown in Table 2. Column bases yield slightly, hence comparison of chord rotations is more meaningful than comparing the plastic rotations. There are no other yielding sections in columns at the upper stories due to the strong column- weak beam condition.

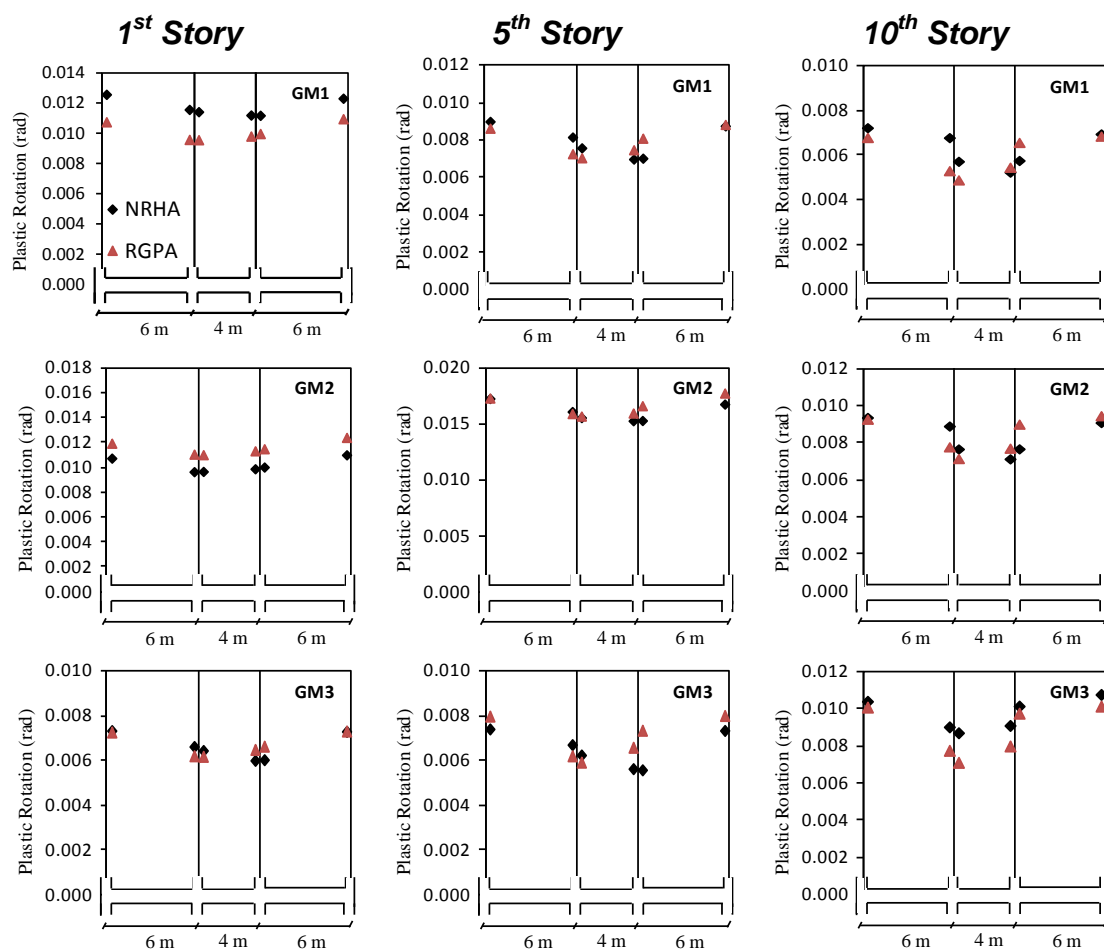


Fig. 9 Beam end plastic rotations when bending moment values at beam ends reach maximum

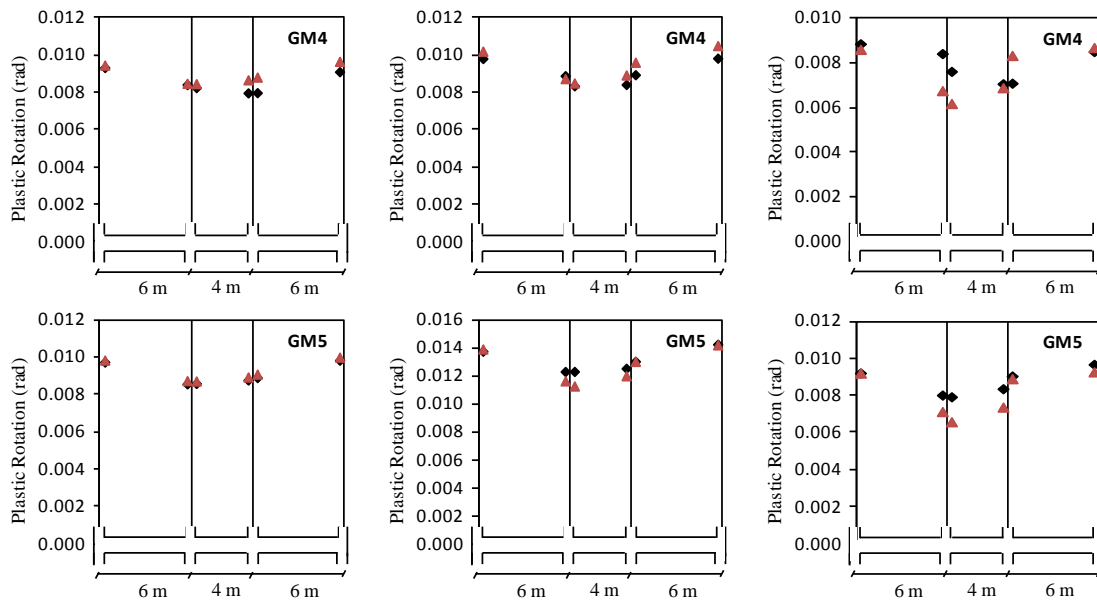


Fig. 9 Continued

Table 2 Maximum average chord rotations of the first story column under six ground motions

Analysis Procedure	Chord Rotations of the First Story Column Bases (rad)					
	GM1	GM2	GM3	GM4	GM5	GM6
NRHA	0.0066	0.0058	0.0040	0.0050	0.0053	0.0061
RGPA	0.0050	0.0069	0.0040	0.0050	0.0049	0.0059
<b>Yield Chord Rotation = 0.0049 rad.</b>						

RGPA almost exactly predicts the beam end moments and shear forces computed by NRHA. Hence the element force results are not presented for brevity. Table 3 shows the yield moment, yield curvature and yield rotation values for each beam type.

Table 3 Yield moment values, yield curvatures and yield rotations for beam ends (tension at top)

Story Range	Beam Dimension	Yield Moment, $M_y$ (kN.m)	$\Phi_y$ (rad/m)	$\theta_y$ (rad)
1-4	300x550 mm	231.5	0.0057	0.0016
5-8	300x500 mm	230.5	0.0063	0.0016
9-12	300x450 mm	170.0	0.0070	0.0016

Plastic rotations at the beam ends given in Fig. 9 and the yield rotations in Table 3 can be used to calculate the rotation ductilities at beam ends. They vary from 5 to 12, indicating significant plastic deformations at the beam ends under all ground motions. This is an expected result for a frame satisfying capacity design principles under a design spectrum reduced with a reduction factor of 8. Plastic deformations occur at the

beam ends with rotation ductilities conforming to the reduction factor, whereas column bases yield only slightly in conformance with the strong column - weak beam principle of capacity design.

The plastic hinge patterns obtained by NRHA and RGPA under GM1 are shown in Fig. 10 below. It can be observed that they are identical. RGPA perfectly predicts the location of plastic hinges.

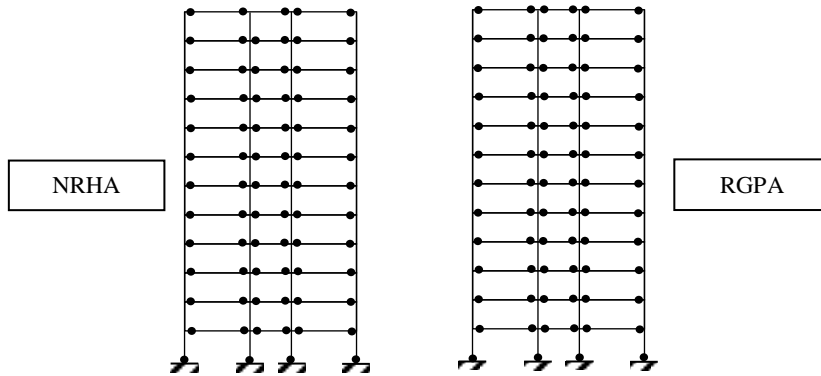


Fig. 10 Plastic hinge patterns under GM1

All analyses presented so far are conducted under synthetic ground motions matching the design spectrum. A final verification analysis is conducted by employing the reference GM4 (CHY006-E) scaled by 1.5 in order to produce larger plastic deformations under an actual ground motion. The comparison of NRHA and RGPA results for the distributions of interstory drift ratio, mean beam plastic rotations and mean column chord rotations are presented in Fig. 11. The distribution of yield interstory drift ratio is also given in the first figure box. These are the values recorded when the first yielding in a beam at any story occurs. It is evident from these figures that interstory drift and rotation ductilities exceed 10 (see  $\theta_y$  in Table 3) and RGPA predictions are quite successful.

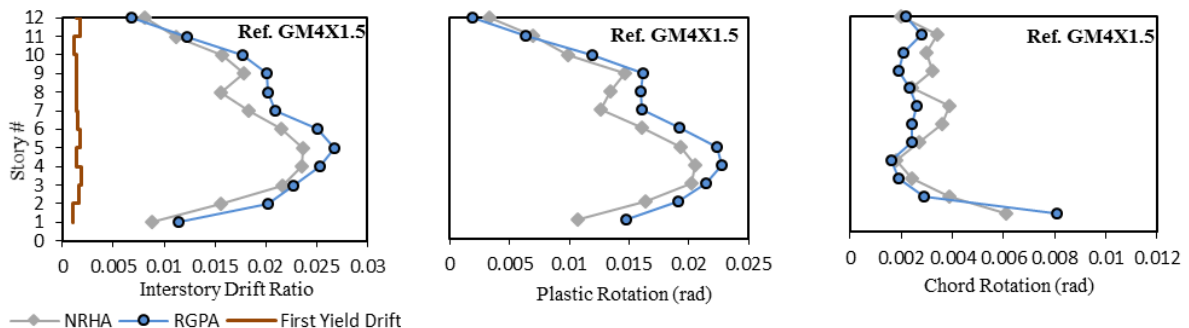


Fig. 11 Interstory drift ratio, mean beam plastic rotations and mean column chord rotations under the actual GM4 scaled by 1.5.

*The 2015 World Congress on*  
**Advances in Structural Engineering and Mechanics (ASEM15)**  
*Incheon, Korea, August 25-29, 2015*

The 20-story RC wall - frame system is analyzed under two variants of the actual ground motion CHY006-E (reference GM4 in Table 1). The first variant is the original, unscaled ground motion and the second variant is obtained by scaling the accelerations of the first variant by 1.5, with the resulting acceleration spectrum shown in Fig. 6. The objective is to test the validity of the proposed procedure under very strong ground excitations producing significant deformation demands far into the plastic range.

The distribution of interstory drift ratios under two ground motions are given in Fig. 13. In addition, maximum average beam-end plastic rotations and maximum average column-end chord rotations are presented for Frame A (with shear wall) in Fig. 14 and Fig. 15, respectively. It can be inferred from the comparison of interstory drift ratios, beam-end plastic rotations and column-end chord rotations that RGPA results are well synchronized with the NRHA results for both ground motions. Column bases yield only slightly under 1.5\*GM4, hence the comparison is presented in terms of chord rotations rather than the plastic rotations. Presence of shear walls reduce the deformation demands from columns significantly, which is an expected result for a code designed frame-wall system.

Table 4 shows the yield moment, yield curvature and yield rotation values for each beam type. RGPA estimates maximum bending moments at the beam ends almost exactly in comparison to the NRHA results. This is repeated for the beam shears, under both ground motions. Hence these results are not presented for brevity.

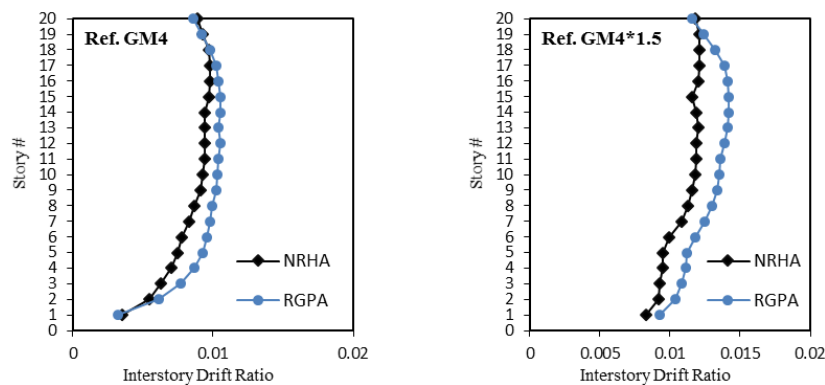


Fig. 13 Comparison of maximum interstory drift ratios

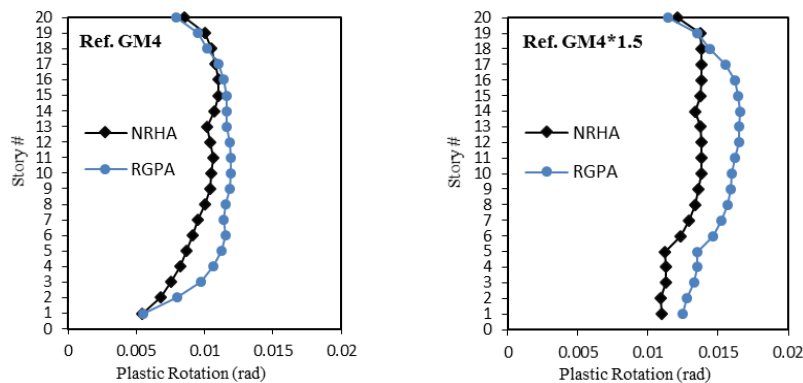


Fig. 14 Comparison of the maximum values of average beam-end plastic rotations in

Frame A

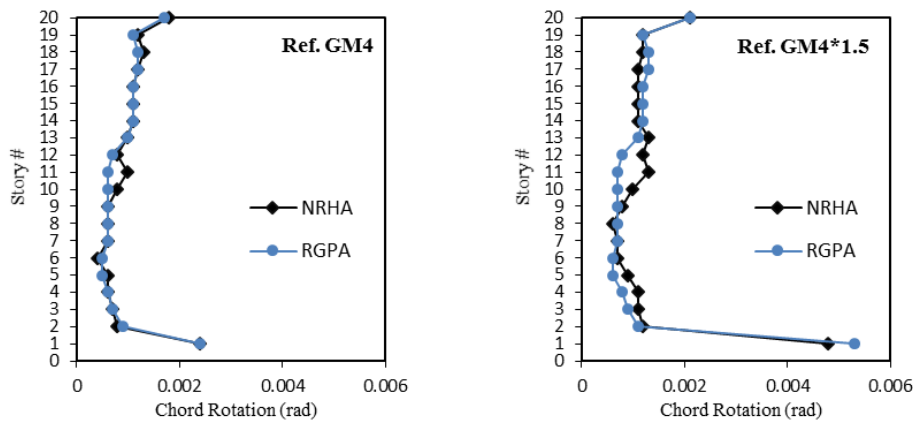


Fig. 15 Comparison of maximum values of average column-end chord rotations in Frame A ( $\theta_{y,base} = 0.0049 \text{ rad}$ )

Average beam plastic rotations given in Fig. 14 reveal that beam rotation ductilities vary between 4 and 7 under GM4, and between 9 and 11 under 1.5\*GM4 in view of Table 4.

Significant plastic rotations at the shear wall occur only at the base. Comparison of plastic rotations from RGPA and NRHA are presented in Fig. 16 below under the original and scaled ground motions. Comparison of maximum bending moments along the shear wall axis in Frame A are also presented in Fig. 17 under GM4 and 1.5\*GM4. Similar to the previous case studies, member internal force results of RGPA are the envelopes of the results obtained by pushing the system in both directions. RGPA estimates maximum moments calculated by NRHA along the wall height quite well although there are differences at the mid height of the wall. The reason is the difference between the plastic deformation sequences. When a plastic hinge forms at the wall base during dynamic response, higher modes become more effective at the mid height and they may cause further plastic deformations at the mid height region during the following time steps. This phenomenon which is called “shear amplification” in shear walls cannot be captured accurately by nonlinear static procedures. This phenomenon is also apparent in Fig. 16 for plastic rotations along the shear wall.

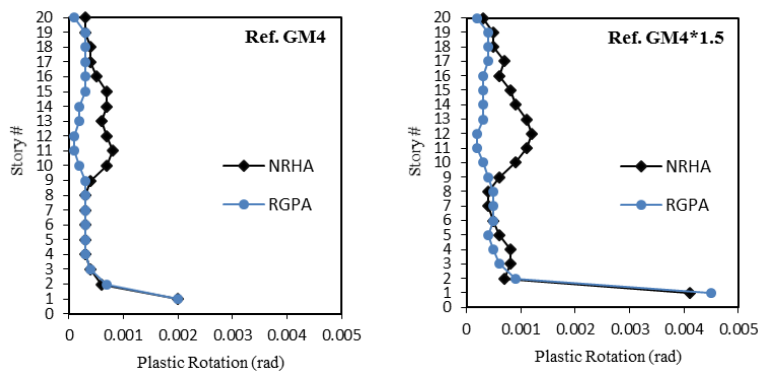


Fig. 16 Comparison of the maximum values of shear wall plastic rotations in Frame A

Table 4 Negative yield moment values for beam ends (tension at top), yield curvatures and yield rotations

Story Range	Beam Dimension	Yield Moment, $M_y$ (kN.m)	$\Phi_y$ (rad/m)	$\theta_y$ (rad)
1-6	300x550 mm	231.5	0.0057	0.0016
7-12	300x500 mm	230.5	0.0063	0.0016
13-20	300x450 mm	204.1	0.0077	0.0017

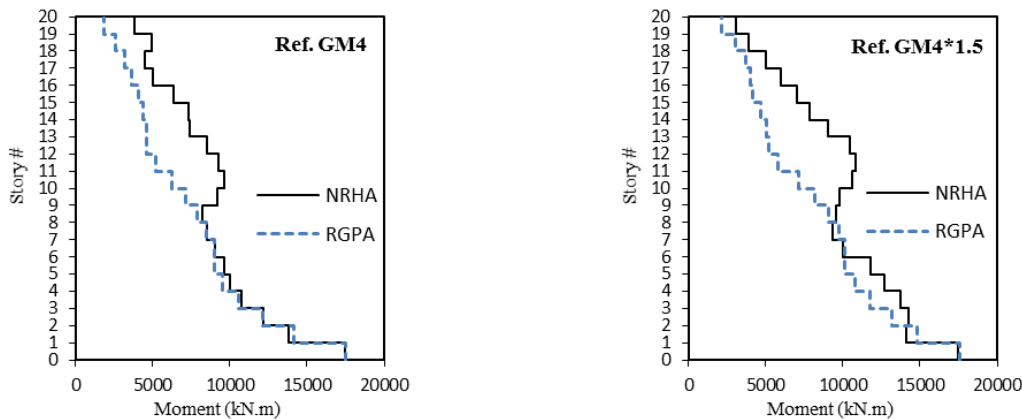


Fig. 17 Maximum bending moment values along the shear wall height in Frame A

## 6. GENERALIZED PUSHOVER ANALYSIS WITH THE MEAN SPECTRUM OF A SET OF GROUND MOTIONS

Generalized pushover analysis is conducted under individual ground motions in the previous sections, and it is verified that RGPA predicts the results of NRHA with reasonable accuracy. Ground motions are usually defined by their response spectra in seismic evaluation and design. In fact, design spectrum represents the statistical average of a set of ground motions that are expected to occur at a given site. Therefore if it can be shown that RGPA results obtained under the mean spectrum of a set of ground motions are sufficiently close to the mean of individual RGPA results obtained under each ground motion in the set, then RGPA can be suggested as an effective tool for seismic analysis under design spectrum.

The set of six spectrum matched ground motions in Table 1 is employed for this purpose where each ground motion has a response spectrum compatible to a design spectrum as shown in Fig. 6. The maximum responses of the 12 story RC frame are calculated under the mean spectrum in Fig. 6 by RGPA, and these results are compared with the mean of individual RGPA and NRHA results obtained under each ground motion in the set. In calculating the target drift under mean spectrum, elastic spectral displacement amplitude  $D_1$  is used for the first mode in Eq. (3) since the mean spectrum can only be defined for the linear elastic spectra of six ground motions, but cannot be defined for their inelastic spectra.

Mean responses from NRHA, RGPA and the responses obtained from RGPA under the mean spectrum for the 12 story frame are presented comparatively in Fig. 18

for interstory drift ratios and beam-end plastic rotations. It is observed that the RGPA results obtained under mean elastic spectrum are very close to the mean of RGPA results obtained under six ground motions separately. These results predict the mean NRHA results quite well. Slight differences between mean RGPA results and RGPA results obtained under mean elastic spectrum is due to using different displacement amplitudes in target drift estimations. Generally, it can be suggested that RGPA results obtained for mean elastic spectrum are well synchronized with the mean RGPA and mean NRHA results for the interstory drift ratios and member end rotations.

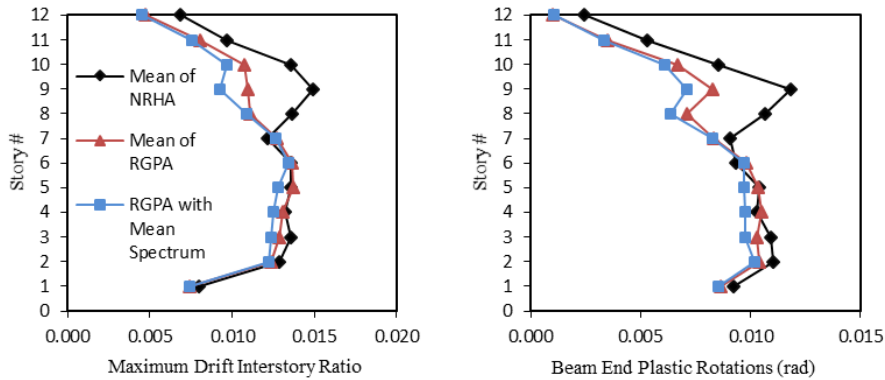


Fig. 18 Comparisons of mean maximum interstory drifts and mean maximum average plastic rotations of beam ends obtained

Mean values of bending moments at beam ends obtained from NRHA, RGPA, and the RGPA results obtained under mean elastic spectrum are presented in Fig. 19 for the 12 story frame. Similar to the previous comparisons, RGPA under mean elastic spectrum captures the mean RGPA values and mean NRHA values almost exactly. Similar results are obtained for Frame A of the 20 story frame-wall system, presented in Fig. 20 below.

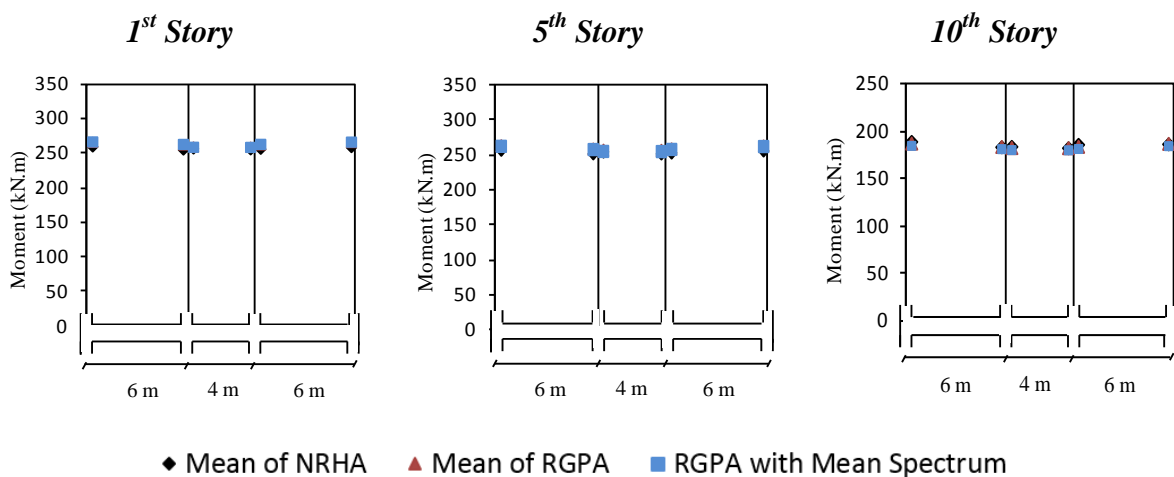


Fig. 19 Comparison of maximum bending moment values of beam ends at the 1st, 5th, and 10th stories

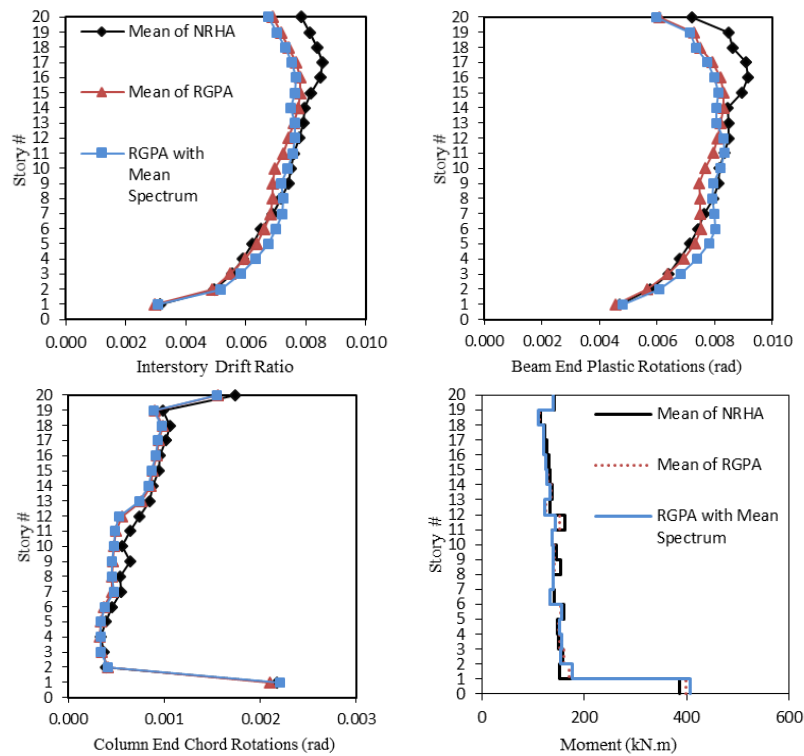


Fig. 20 Comparison of the mean maximum interstory drifts, average plastic rotations of the beam-ends, column-end chord rotations and column moments

## 6. CONCLUSION

The reduction procedure proposed in this study reduces the number of generalized pushovers significantly, from  $N+1$  to  $2^{(n-1)} + 1$  where  $n$  is the number of significant modes and 1 stands for the additional modal pushover for calculating the inelastic spectral displacement at the first mode. When the strong motion intensity is defined by a linear elastic design spectrum, then the required number of generalized pushovers is  $2^{(n-1)} = 4$  for  $n = 3$  significant modes. An additional modal pushover for calculating the inelastic spectral displacement is usually not required for this case since the first mode elastic spectral displacement is calculated from the equal displacement rule.

Practical implementation of generalized force vectors for multi-mode pushover analysis by using the proposed reduction procedure is a much simpler inelastic seismic analysis method compared to nonlinear time history analysis. Yet, it provides quite accurate estimation of internal deformations and almost exact prediction of internal forces calculated by nonlinear time history analysis.

The basic limitation of the RGPA procedure is related to the local accumulation of plastic deformations during actual dynamic response which leads to significant changes in the modal deformation shapes. The non-adaptive RGPA algorithm cannot track these changes and hence its results deviate from the results of nonlinear response history analysis when such localized nonlinearities occur.

## REFERENCES

- Antoniou S. and Pinho R. (2004), "Development and Verification of a Displacement-Based Adaptive Pushover Procedure", *Journal of Earthquake Engineering*, **8**(5), 643-661.
- Aydinoğlu N.M. (2003), "An Incremental Response Spectrum Analysis Procedure Based on Inelastic Spectral Displacements for Multi-Mode Seismic Performance Evaluation", *Bulletin of Earthquake Engineering*, **1**, 3-36.
- Chopra A.K. and Goel R.K. (2002), "A Modal Pushover Analysis Procedure for Estimating Seismic Demands for Buildings", *Earthquake Engineering and Structural Dynamics*, **31**, 561-582.
- Gupta B. and Kunnath S. K. (2000), "Adaptive Spectra-Based Pushover Procedure for Seismic Evaluation of Structures", *Earthquake Spectra*, **16**(2), 367-391.
- Hancock, J. and Bommer, J.J. (2006), "Using Spectral Matched Records to Explore the Influence of Strong-Motion Duration On Inelastic Structural Response", *Soil Dynamics and Earthquake Engineering*, **27**, 291-299.
- Hancock, J., Watson-Lamprey, J., Abrahamson, N.A., Bommer, J.J., Markatis, A., McCoy, E. and Mendis, R. (2006), "An Improved Method of Matching Response Spectra of Recorded Earthquake Ground Motion Using Wavelets", *Journal of Earthquake Engineering*, **10**, Special Issue 1, 67-89.
- Jan T.S., Liu M.W. and Kao, Y.C. (2004), "An Upper-Bound Pushover Analysis Procedure for Estimating the Seismic Demands of High-Rise Buildings", *Engineering Structures*, **26**(1), 117-128.
- Jerez S. and Mebarki A. (2011), "Seismic Assessment of Framed Buildings: A Pseudo-Adaptive Uncoupled Modal Response Analysis", *Journal of Earthquake Engineering*, **15**(7), 1015-1035.
- Kreslin M. and Fajfar P. (2012), "The Extended N2 Method Taking into Account Higher Mode Effects in Elevation", *Earthquake Engineering and Structural Dynamics*, **40**, 1571-1589.
- Kunnath, S.K. (2004), "Identification of Modal Combinations for Nonlinear Static Analysis of Building Structures", *Computer Aided Civil Infrastructure Engineering*, **19**(4), 246-259.
- Matsumori, T., Otani, S., Shiohara, H. and Kabayesawa, T. (1999), "Earthquake Member Deformation Demands in Reinforced Concrete Frame Structures", *Proc. US-Japan Workshop on Performance Based Earthquake Engineering*, PEER Report, University of California, Berkeley.
- Ministry of Public Works and Settlement (2007), *Turkish Earthquake Code: Specifications for Buildings in Disaster Areas*, Ankara, Turkey.
- OpenSees. *Open System for Earthquake Engineering Simulation* (2011). Available from: <http://opensees.berkeley.edu>.
- PEER Strong Motion Database (2010). Available from: <http://peer.berkeley.edu/smcat>.
- Poursha M., Khoshnoudian F. and Moghadam A.S. (2009), "A Consecutive Modal Pushover Procedure for Estimating the Seismic Demands of Tall Buildings", *Engineering Structures*, **31**, 591-599.
- Sucuoğlu H. and Günay M. S. (2011), "Generalized Force Vectors for Multi-Mode Pushover Analysis", *Earthquake Engineering and Structural Dynamics*, **40**, 55-74.